Cellular Physiology and Biochemistry

Cell Physiol Biochem 2018;46:1042-1054
DOI: 10.1159/000488835
Published online: April 18, 2018
Accepted: February 27, 2018

Original Paper

CaMKII Potentiates Store-Operated Ca^{2+} Entry Through Enhancing STIM1 Aggregation and Interaction with Orai1

Shu Li Jingyi Xue Zhipeng Sun Tiantian Liu Lane Zhang Limin Wang Hongjie You Zheng Fan Yuanyuan Zheng Dali Luo

Department of Pharmacology, School of Basic Medical Sciences, Capital Medical University, Beijing, P.R. China

Key Words
CaMKII • Store-operated Ca^{2+} entry • STIM1 • Orai1

Abstract
Background/Aims: Upon Ca^{2+} store depletion, stromal interaction molecule 1 (STIM1) oligomerizes, redistributes near plasmalemma to interact with Ca^{2+} selective channel-forming subunit (Orai1) and initiates store-operated Ca^{2+} entry (SOCE). Ca^{2+}/calmodulin-dependent protein kinase II (CaMKII) is a regulator of SOCE, but how CaMKII regulates SOCE remains obscure. ***Methods:*** Using Fura2, confocal microscopy, co-immunoprecipitation, specific blocker and overexpression/knockdown approaches, we evaluated STIM1 aggregation and its interaction with Orai1, and SOCE upon Ca^{2+} store depletion in thapsigargin (TG) treated HEK293 and HeLa cells. ***Results:*** Overexpression of CaMKIIδ enhanced TG-induced STIM1 co-localization and interaction with Orai1 as well as SOCE. In contrast, CaMKIIδ knockdown and a specific inhibitor of CaMKII suppressed them. In addition, overexpression or knockdown of CaMKIIδ in TG treated cells exhibited increased or reduced STIM1 clustering and plasmalemma redistribution, respectively. ***Conclusion:*** CaMKII up-regulates SOCE by increasing STIM1 aggregation and interaction with Orai1. This study provides an additional insight into SOCE regulation and a potential mechanism for CaMKII involvement in some pathological situations through crosstalk with SOCE.

Introduction

Store-operated Ca^{2+} entry (SOCE) is a common Ca^{2+} entry mode in excitable and non-excitable cells. This Ca^{2+} influx not only delivers Ca^{2+} to refill sarcoplasmic/endoplasmic reticulum (SR/ER) Ca^{2+} stores after depletion, but also acts as a Ca^{2+} signal to regulate a variety of cellular events, including gene expression, cell growth, proliferation, migration and apoptosis [1-4]. It is well accepted that the assembling of stromal interaction molecule 1

S. Li and J. Xue contributed equally to this work.

Dali Luo
Department of Pharmacology, Capital Medical University,
District of Feng Tai, Street of Youanmenwai, #10 Xi TouTiao, Beijing (P.R. China)
Tel. +86-10-83911517, Fax 86-10-83911517, E-Mail luodl@ccmu.edu.cn

(STIM1) towards Ca^{2+} selective channel-forming subunit (Orai1) in plasma membrane (PM) is the fundamental mechanism to drive SOCE. Upon depletion of ER Ca^{2+} stores, STIM1 senses the lowered ER Ca^{2+} levels via its luminal Ca^{2+}-binding E-F hand, and then oligomerizes and translocates to membrane contact junctions between the ER and the PM, thus displaying distinct STIM1 puncta. At the same time, Orai1 accordingly redistributes in the PM and interacts with STIM1 to trigger SOC channel opening [5, 6].

Although the basic molecular mechanisms of SOCE activation and the contributing proteins are well understood, the regulatory mechanisms involving the interaction of STIM1 with Orai1 and the fine-tuned modulation of SOCE are quite complicated and far from clear [7]. Several regulators of STIM1/Orai1 complex, such as septins, surfeit locus protein, Ca^{2+} release-activated Ca^{2+} channel regulator and store-operated Ca^{2+} entry-associated regulatory factor, have been proposed [8-11]. We also find a down-regulatory mechanism for SOCE through calsequestrin-1, a Ca^{2+} binding protein inside SR/ER, interacting with STIM1 [12, 13]. In addition, calmodulin (CaM) and kinases including mitogen-activated protein kinase and AMP-activated protein kinase have been demonstrated to affect Orai1 and STIM1 phosphorylation and the following SOCE [14-16].

Ca^{2+}/CaM-dependent protein kinase II (CaMKII) represents a family of serine/threonine (Ser/Thr) protein kinases encoded by four different genes called CaMKIIα, β, γ and δ, which exist as an assembly of monomers found in different tissues. When Ca^{2+} rises, Ca^{2+}/CaM binds to the regulatory segment of CaMKII and triggers its conformational change, making Thr287 available for phosphorylation for CaMKII activation [17, 18]. CaMKII is a paramount regulator of multiple Ca^{2+} handling proteins and ion channels. In physiological conditions, CaMKII activation leads to increases in the open probability and Ca^{2+} window current via phosphorylating ryanodine receptor [19] and L-type Ca^{2+} channel [20]. Its activation also inhibits Ca^{2+} uptake into the SR via phosphorylation of phospholamban and inhibition of SR Ca^{2+}-pump ATPase [21]. Under pathological settings, CaMKII has been implicated to be involved in melanoma cell migration/metastasis [4], cardiomyocyte hypertrophy [22] and neointima formation after vascular injury [23] through SOCE. However, the exact role of CaMKII in regulation of SOCE remains largely unknown. Here, we found that CaMKII up-regulates SOCE through enhancing STIM1 aggregation near PM and interaction with Orai1 upon stores depletion in HEK293 cells and HeLa cells, two cell lines widely used in the investigation of SOCE.

Materials and Methods

Reagents and antibodies

Lipofectamine 2000, rProtein G beads, Fura2-AM, Alexa Fluor dye-conjugated secondary antibodies were purchased from Life Technology. Phospho-CaMKII pThr287 antibody (MA1-047) and Super Signal West Pico enhanced chemiluminescence reagents kit were from Thermo Scientific (MA, USA). Rabbit polyclonal CaMKII delta antibody (GTX111401) was from Gene Tex, Inc (CA, USA). Thapsigargin (TG), formaldehydrate solution, and protease inhibitor cocktail were from Sigma-Aldrich (St. Louis, MO, USA). KN-93 and KN-92 were from Merck Millipore (Billerica, MA, USA). Anti-phosphoserine antibody (Ab17465) was from Abcam (Cambridge, USA). All of the antibodies including mouse monoclonal anti-GAPDH (sc-365062), mouse monoclonal anti-STIM1 (SC-166840), rabbit polyclonal anti-STIM1 (SC-68897), mouse monoclonal anti-Orai1 (SC-377281), goat anti-mouse IgG-HRP (SC-2005) and goat anti-rabbit IgG-HRP (SC-2004) were from Santa Cruz Biotechnology, Inc. (Santa Cruz, CA, USA). Anti-HA was bought from Cell Signal Tech (CST3724T).

Cell culture

HEK293 cells and HeLa cells were obtained from ATCC and were cultured at 37°C in Dulbecco's modified Eagles medium (DMEM, Gibco, Rockville, MD, USA) containing 10% fetal bovine serum (FBS, Hyclone, AUS) in humidified 95% air and 5% CO_2 incubators.

Plasmids and cell transfection

Plasmids were constructed by ViGene Biosciences Inc. (Rockville, MD, USA). Overexpression of HA-tagged *human CaMKIIδ* was generated by PCR. Each cDNA was cloned into the pDEST-EGFP expression vector and HA-tag was inserted into C-terminal of CaMKII. HEK293 cells and HeLa cells were transfected with *CaMKIIδ* through Lipofectamine 2000 reagent as previously described [12].

Small interfering RNA-based experiment

Small interfering RNAs (siRNAs) targeting *CaMKIIδ* gene was designed and synthesized by Invitrogen (Carlsbad, CA, USA), and the effect of CaMKIIδ-siRNA was identified by Western blot. The sense sequence of siRNA is as follows: 5′-GGGAUGGAUUUUCACCGAUtt-3′. Scrambled RNA oligonucleotides were used as control. HEK293 cells and HeLa cells in 6 cm dishes were transfected with 40 nM siRNA oligonucleotides using Lipofectamine 2000 reagent (Invitrogen, Life Technologies) according to the manufacturer's instructions. The medium was replaced with Dulbecco's Modified Eagle's medium containing 10% fetal bovine serum after 8 h, and cells were further cultured for 48 h.

Co-immunoprecipitation and western blotting

Co-immunoprecipitation was carried out as previously described [12]. Western blotting was performed as following: The extraction of cell protein was prepared by washing the cells with phosphate-buffered saline (PBS) and then lysing the cells in RIPA buffer, containing 1 mM PMSF and protease inhibitor cocktail for 30 min on ice. Protein samples were heated by incubation in loading buffer for 5 min at 95°C, resolved on a 10% SDS-PAGE and transferred to nitrocellulose membranes. The membranes were subsequently blocked for 1 h at room temperature in 5% non-fat milk. The primary antibodies used for STIM1, Orai1, CaMKIIδ, p-CaMKII at Thr287, and GAPDH were at ratio of 1:1000, 1:500, 1:1000, and 1:1000, 1:1500, respectively, with an overnight incubation at 4°C. The horseradish peroxidase-conjugated secondary antibodies were all diluted at 1:1000 with room temperature for 1 h. Immunoreactive bands were exposed using enhanced chemiluminescence reagents and intensity of each band was normalized with GAPDH.

Immunofluorescence

Cells were plated on 5 x 5 mm cover slides in 6 well plates (5 x 10^4 cells per well). After 24 h culture and plasmids transfected for 48 h, the cells stimulated with 1 μM thapsigargin (TG) plus 2 μM ionomycin for 5 min in Ca^{2+}-free medium (the addition of ionomycin can cause more obvious STIM1 conformation and co-locolization with Orai1 observed by microscope [12]), and were fixed in PBS containing 4% paraformaldehyde for 20 min. Then cells were permeabilized by 0.1% Triton X-100 in PBS for 30 min and blocked in 5% bovine serum albumin for 1 h at room temperature. The anti-STIM1, anti-Orai1 and anti-HA antibodies were used at a dilution of 1:50, 1:50, and 1:1000, and the secondary antibody Alexa Fluor 594-labeled goat anti-mouse and Alexa Fluor 488-labeled donkey anti-rabbit used at a dilution of 1:750, respectively. Hoechst 33342 was used to label the nucleus for 10 min at room temperature. The laser-scanning confocal microscope was used to detect the chemifluorescent as previously described [12, 13]. After mounting, a 3-D z-stack was obtained at 0.5 μm intervals by Leica SP8 microscopy equipped with a 63x oil immersion objective (NA 1.4), pinhole=1.0 μm for measurement of co-localization of STIM1 with Orai1. The Pearson's coefficient values that represent the degree of co-localization were categorized as strong (0.49–1.0), moderate (0.1–0.48) and weak (−1 to 0.09) based on previous description [24, 25].

Measurement of cytosolic Ca^{2+} concentration and Mn^{2+} quenching

The procedures of intracellular Ca^{2+} concentration ($[Ca^{2+}]_i$) and Mn^{2+} quenching measurements were carried out as previously described [12, 26]. For drug treatment, KN-93 was presented during the cell washes and incubation in Ca^{2+}-free medium for 10 min before TG treatment. Values of $[Ca^{2+}]_i$ was calculated by using the FL Solutions Intracellular Cation Scan software, and values of Mn^{2+} quenching was expressed as the percentage of the initial fluorescence value in the absence of extracellular Mn^{2+} [12, 26]. Hepes-buffered saline solution (HBSS) contained (mM): NaCl, 120; KCl, 5.4; Mg_2SO_4, 0.8; HEPES, 20; $CaCl_2$, 1.8; and glucose, 10; with pH 7.4 adjusted by NaOH). Ca^{2+}-free solutions contained no added $CaCl_2$ with 1 mM EGTA in the HBSS.

Chemical cross-linking

HEK293 cells were detached by centrifugation at 200 g for 1 min and resuspended in HBSS. Cells were then cross-linked with 1% (w/v) formaldehyde solution for 5 min. The cross-linking reaction was terminated with a final concentration of 0.1 M glycine stock solution and the incubation was continued for 5 min at 4°C. After centrifuging at 200 g for 1 min and washing 3 times with ice-cold HBSS, cells were lysed with lysis buffer, containing 1% SDS, 0.1% Triton-X100, 1 mM PMSF and protease inhibitor cocktail under constant agitation at 4°C for 5 min. Then the lysates were centrifuged at 4°C, 15000 g for 15 min and the supernatants were collected for Western blotting without boiling before loading in the comb hole based on previous description [12, 27].

Statistical analysis

All data present as means ± SD, and n indicates independent experiments. Statistical analyses in each response were performed using Student's t-test or one-way analyses of variance (ANOVA). $P<0.05$ was considered statistically significant.

Results

Inhibition of CaMKII attenuates SOCE

SOCE was induced in Fura2 loaded cells by thapsigargin (TG, 1 μM) in Ca^{2+}-free medium for 5 min followed by Ca^{2+} addition into the medium. Pretreatment of the cells with 5 or 10 μM KN93 for 10 min, to block CaMKII [17-21], significantly inhibited the first peak and the following plateau of Ca^{2+} influx induced by TG in both HEK293 (Fig. 1A and B) and HeLa cells (Fig. 1D and E), while the Ca^{2+} release phase remained unaltered. The relative Ca^{2+} entry

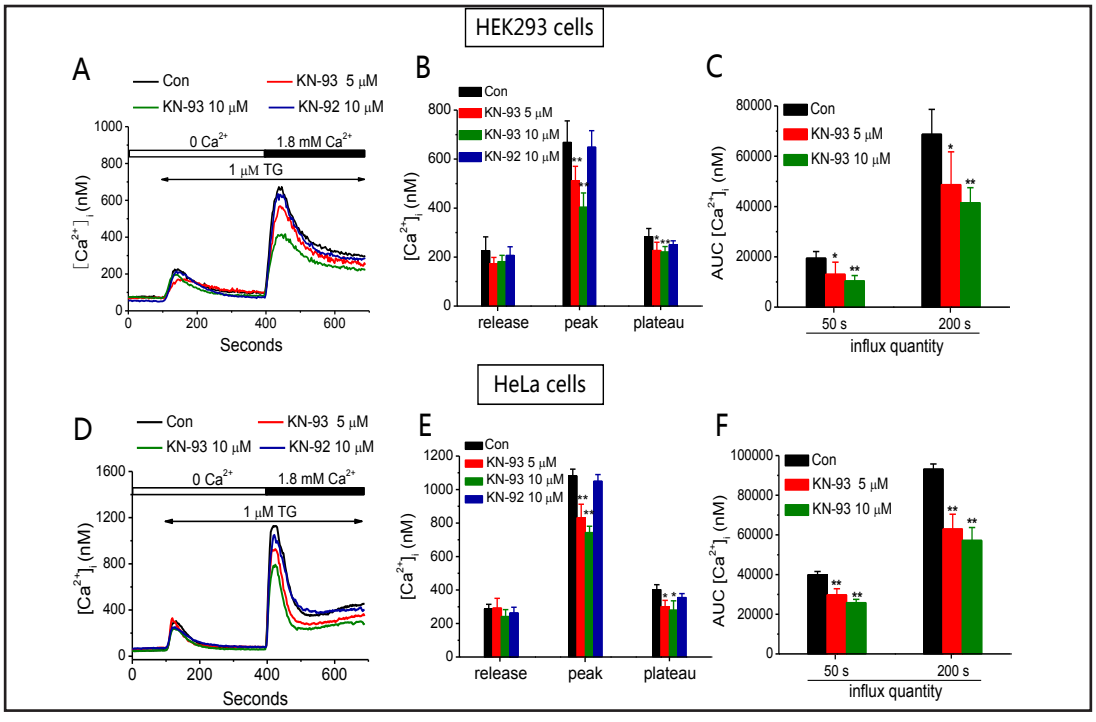

Fig. 1. Effect of CaMKII inhibition on SOCE in HEK293 cells and HeLa cells. (A and F) Typical curves show the protocol of SOCE measurement in cells loaded with Fura2. After pretreatment of cells with KN-93 (5 or 10 μM) or KN-92 (10 μM) for 10 min in HEK293 (A-C) and HeLa cells (D-F), Ca^{2+} release in Ca^{2+}-free solution and Ca^{2+} influx following the addition of 1.8 mM Ca^{2+} were induced by TG. Statistical data show the average peaks±SD of Ca^{2+} release, Ca^{2+} influx peak and plateau (at 700 s, B and E), and SOCE quantity within the initial 50 s or 200 s in response to TG (C and F). N=5-6 independent experiments for each bar. * and ** represent $P<0.05$ and $P<0.01$ vs. control, respectively, analyzed by Student's t-test.

quantity obtained by calculating the areas under 50 s and 200 s curves after re-addition of Ca^{2+}, representing the fast and slow Ca^{2+} entry phase respectively [12], were also decreased because of KN93 treatment (Fig. 1C and F). However, the pretreatment of cells with KN92 (10 μM), an inactive chemical analog of KN93, showed no effect on SOCE.

Furthermore, SOCE was assessed by quenching the intracellular Fura2 fluorescence via the entry of extracellular Mn^{2+} to eliminate possible influence of Ca^{2+} transport mechanism. Compared with control, the maximum Mn^{2+} quenching due to TG was significantly reduced in the presence of 10 μM KN93, but not 10 μM KN92 (Fig. 2A and B). As CaMKIIδ is widely expressed in various tissues, and its activation is manifested by phosphorylation at Thr287 [17-19], we then detected CaMKIIδ activity by assessing Thr287 phosphorylation with a specific antibody. TG treatment could promote CaMKII phosphorylation at Thr287, while pretreatment of cells with KN-93 at the concentration inhibiting SOCE prevented the increased Thr287 phosphorylation due to TG in both types of cells (Fig. 2C and D). Therefore, these results may suggest that the endogenous CaMKII is activated upon TG stimulation, and as a result, is involved in the regulation of SOCE in both HEK293 and HeLa cells.

Change in CaMKII expression affects SOCE

To further address the issue of CaMKII activity on SOCE, we determined the effects of knocking down the endogenous CaMKIIδ and increasing its expression on SOCE. The abundance of CaMKIIδ expression in HEK293 and HeLa cells interfered with CaMKIIδ-siRNA or transfected with plasmid encoding HA-tagged human wild-type *CaMKIIδ* gene were examined. By detecting the green fluorescent protein, we found a >90% transfection efficiency in both HEK293 and HeLa cells treated with the plasmid at concentration of 2 μg/ml for 48 h, thus, we used this concentration in all the following examinations. Compared with counterpart controls, cells treated with CaMKIIδ-siRNA displayed a significant decrease in CaMKIIδ expression (46.3±14.2% of control), while cells transfected with *CaMKIIδ-wt* showed an approximately a 6-fold increase in CaMKIIδ expression; STIM1 and Orai1 expressions remained unchanged in both CaMKIIδ manipulated cells (Fig. 3A and B). Accordingly, compared with control cells, the peak, the plateau and the relative quantity of Ca^{2+} influx induced by TG were significantly inhibited in CaMKIIδ knockdown but enhanced in CaMKIIδ overexpressed HEK293 cells (Fig. 3C-E) and HeLa cells (Fig. 3F-H), while their Ca^{2+} release phases were not affected. Here, we used 0.5 μM TG, because the potential effect of CaMKII on SOCE was

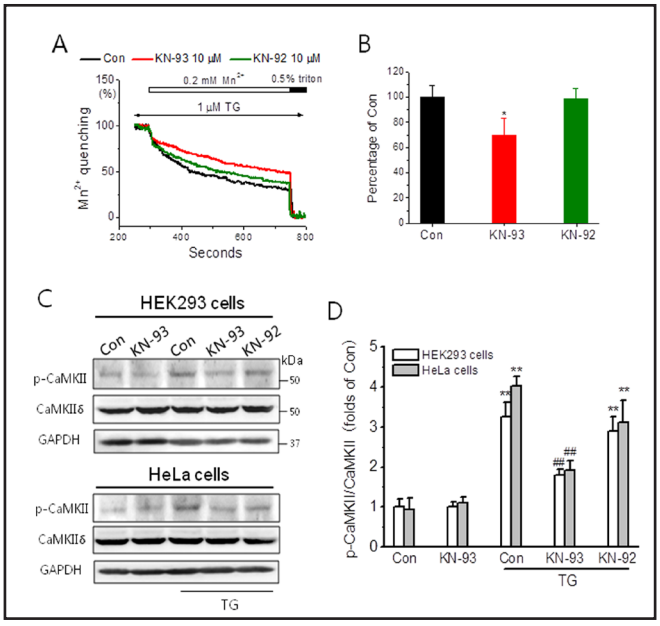

Fig. 2. Effect of CaMKII inhibition on Mn^{2+} influx and CaMKIIδ phosphorylation induced by TG. (A and B) Typical curves illustrate the effect of KN-93 (10 μM) and KN-92 (10 μM) pretreated HEK293 cells for 10 min on TG-induced Mn^{2+} influx in Ca^{2+}-free medium (A), and the average rate of Mn^{2+} quench, expressed as the percentage of the initial fluorescence value in the absence of extracellular Mn^{2+}, for each condition±SD from 4 independent experiments (B). (C and D) The expression levels of p-CaMKIIδ at Thr287 and total CaMKIIδ were detected by Western blot using specific antibodies (C) and their statistical date (D) in 4 independent experiments. * and ** represent P<0.05 and P<0.01 vs. control (H_2O), respectively. ##P<0.01 vs. control with TG, analyzed by Student t test (B) and one-way ANOVA test (D).

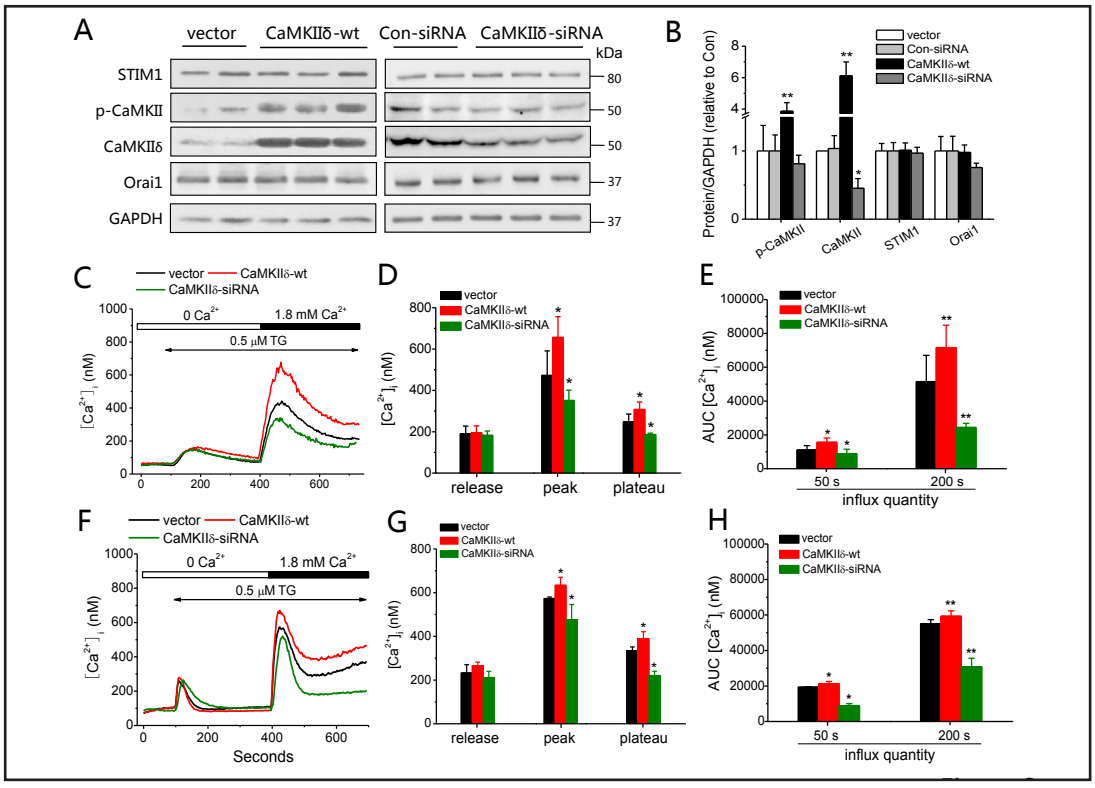

Fig. 3. Effect of CaMKIIδ knockdown and overexpression on SOCE. (A and B) Typical labeling bands (A) and expression levels (B) of CaMKIIδ phosphorylation at Thr287, CaMKIIδ, STIM1 and Orai1 by Western blot using specific antibodies in HEK293 cells transfected with vector or CaMKIIδ-wt, or treated with CaMKIIδ-siRNA or Con-siRNA for 48 h are showed. n=3-4 independent experiments. (C-H) Representative traces in HEK293 (C) and HeLa cells (F) show the effects of CaMKIIδ overexpression and knockdown on SOCE induced by TG. Statistical data show the average peaks±SD of Ca^{2+} release and Ca^{2+} influx peak phase and plateau phase (at 700 s), and SOCE quantity within the initial 50 s and 200 s in response to TG as indicated in HEK293 (D and E) and HeLa cells (G and H). N=5-6 independent experiments for each bar. * and ** represent P<0.05 and P<0.01 vs. vector or Con-siRNA, respectively, analyzed by Student's t-test.

more significant in 0.5 μM than 1 μM TG treated cells, especially for HeLa cells. Similarly, the rate of Mn^{2+} quenching was also promoted in CaMKIIδ overexpressed cells and decreased in CaMKIIδ deficient cells (data not shown). Thus, the effect of manipulating CaMKIIδ expression supports the notion that CaMKII activation up-regulates SOCE.

CaMKII affects STIM1 interaction with Orai1

It is well accepted that upon store depletion, STIM1 oligomerizes, translocates to the ER-PM contact junctions, and interacts with Orai1 to trigger SOC channel opening [5-7]. Thus, STIM1 and Orai1 association was measured by evaluating STIM1 co-localization with Orai1 in whole cell using Imaris Bitplane software. This quantitative measurement can give an overlap degree presented by the Pearson correlation coefficient between fluorescence signals acquired in two channels [12, 13, 24-26]. We found an approximately 2-fold increase in STIM1 and Orai1 co-localization on PM of cells after TG (1 μM)+ionomycin (2 μM)-treatment for 5 min in Ca^{2+}-free medium compared with control cells, but this increased co-localization was prevented by pretreatment of the cells with KN-93, but not with KN-92 (Fig. 4A and B). In contrast, CaMKIIδ-overexpression cells treated with TG exhibited an increase in the Pearson correlation coefficient of STIM1/Orai1 compared with that of control cells (Fig. 4C and D). To avoid the variation in cells selection for 3-D scanning and calculation of Pearson coefficient, here we added ionomycin because more uniformed STIM1 oligomerization and

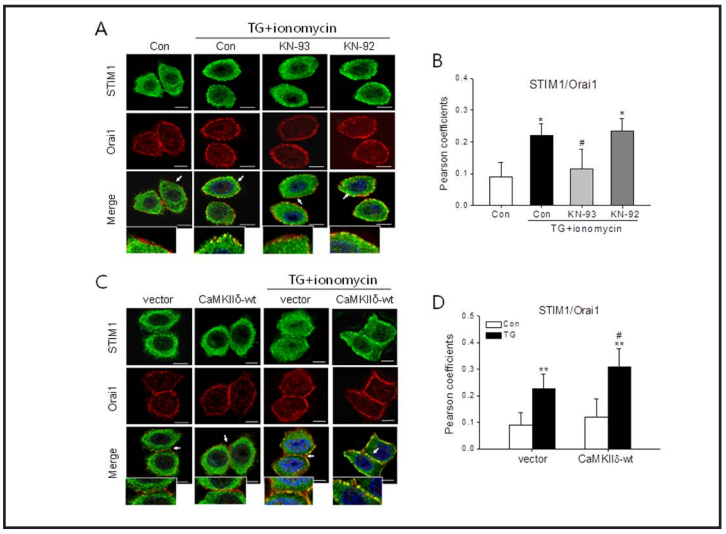

Fig. 4. Effect of CaMKII on STIM1/Orai1 co-localization. The subcellular distribution of STIM1 and Orai1 were detected by double immunostaining HeLa cells with specific antibody for STIM1 or Orai1. The nucleus was labeled with Hoechst33342 (1 μg/ml). Scale bar=10 μm. (A and C) The co-localization of STIM1 and Orai1 in cells pretreated with KN-93 (10 μM) or KN-92 (10 μM) for 10 min (A), or transfected with CaMKIIδ-wt for 48 h (C) was visualized under confocal microscope (see Methods). (B and D) The graph bars illustrate the Pearson correlation coefficients±SD in response to TG (1 μM)+ionomycin (2 μM) treatment for 5 min in Ca^{2+}-free medium, n=30–40 cells for each bar. * and ** represent P<0.05 and P<0.01 vs. control or vector, respectively. #P<0.05 vs. control or vector with TG, analyzed by one-way ANOVA test.

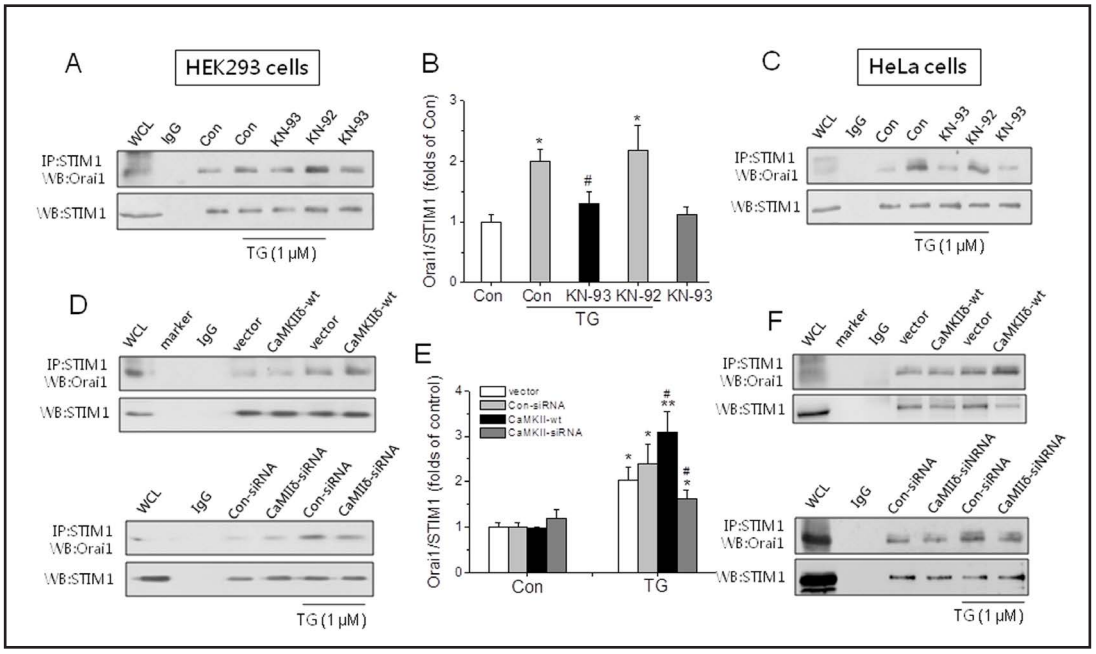

Fig. 5. Effect of CaMKII on the STIM1/Orai1 physical interaction. (A-C) Typical blotting bands show the effect of KN93 on the association of STIM1 with Orai1. HEK293 cells (A and B) and HeLa cells (C) were preincubated with 10 μM KN93 or KN92 for 10 min, incubated in Ca^{2+}-free HBSS for 5 min and stimulated with 1 μM TG for 5 min in Ca^{2+}-free medium. Then the whole cell lysates were immunoprecipitated with anti-STIM1 mAb and protein-G agarose, and Western blot was performed with anti-Orai1 mAb. The STIM1/Orai1 association intensities were quantified as average protein ratios±SD of Orai1/STIM1 (B). (D-F) Effects of CaMKIIδ knockdown by siRNA and CaMKIIδ overexpression by CaMKIIδ-wt for 48 h on the association of STIM1 with Orai1 in HEK293 (D and E) and HeLa cells (F) with the similar protocol as described in A and B. n=3-4 independent experiments for each bar. * and ** represent P<0.05 and P<0.01 vs. vector or Con-siRNA without TG, respectively. #P<0.05 vs. vector or Con-siRNA with TG, respectively, analyzed by one-way ANOVA test.

translocation near PM was found in most of the cells in a dish than 1 μM TG stimulated alone [28, 29].

To further verify the influence of CaMKII on the association of STIM1 with Orai1, we carried out co-immunoprecipitation experiment using specific antibody for STIM1 or Orai1. We found that STIM1 co-immunoprecipitated with Orai1 after TG stimulation for 5 min, and this interaction was partially prevented due to the pretreatment of cells with KN-93, but not with KN-92, at the concentration inhibiting Ca^{2+} entry (Fig. 5A-C). Knocking down the endogenous CaMKIIδ expression reduced STIM1/Orai1 physical interaction, whereas overexpressing CaMKIIδ increased their association after TG stimulation in both types of cells (Fig. 5D-F).

CaMKII enhances STIM1 aggregation

To further investigate how CaMKII regulates SOCE, STIM1 aggregation and trafficking towards cell surface upon store depletion were examined by immunostaining STIM1 alone to avoid possible influence of Orai1 labeled fluorescence and calculating STIM1 puncta at the size of 0.5-1 μm that are usually taken as STIM1 aggregation when store depleted [5-7, 30]. We calculated the STIM1 clusters in whole cell (excluding the nuclear area) and the perimembranous region (from membrane surface to 1.0 μm inside) using Imaris Bitplane software in cells from 3-D stack images (Fig. 6A) [12, 13]. A dramatic increase in STIM1 clustering in whole cell and, in particular, the perimembranous area (16.5 times vs. 8.9 times in cytosolic area) was found after TG stimulation. While pretreatment of the cells with KN-93 or CaMKIIδ-siRNA reduced STIM1 clustering in both areas, CaMKIIδ overexpression significantly increased the STIM1 aggregation upon store depletion (Fig. 6A and B). Moreover, to avoid possible interference of the non-transfected cells that might be mistaken as CaMKIIδ-positive cells, double-staining the overexpressed cells with antibodies against HA-CaMKIIδ and STIM1 was carried out. Subconfluent (used in the measurements of internal Ca^{2+} and

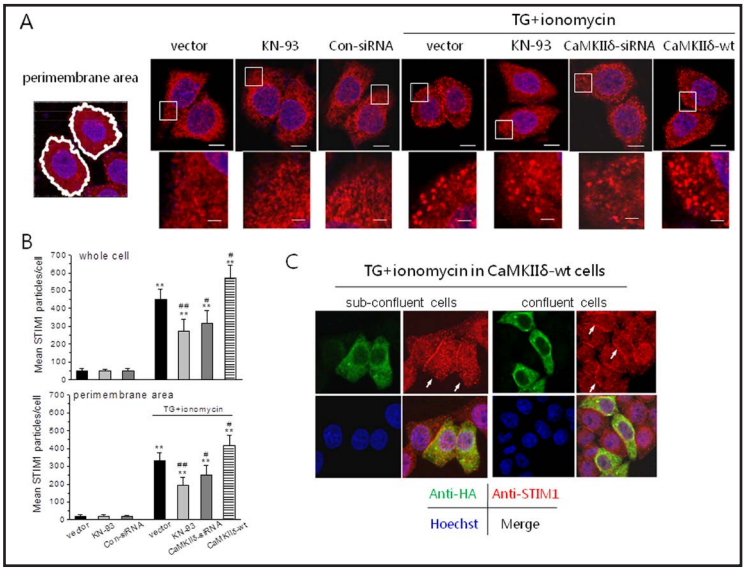

Fig. 6. Effect of CaMKII on STIM1 oligomerization and aggregation. (A) The 2-D image in left defines the localization and scope of STIM1 particles after TG (1 μM)+ionomycin (2 μM) treatment counted within the perimembranous area (from cell surface to 1 μm inside) as indicated with white circle. The images in right illustrate STIM1 aggregation and redistribution after Ca^{2+} store depletion by TG+ionomycin for 5 min in Ca^{2+}-free medium in HeLa cells that had been treated with KN-93 (10 μM) for 10 min, CaMKIIδ-wt, vector, CaMKIIδ-siRNA or Con-siRNA for 48 h, as indicated. The counting of STIM1 particles (0.5～1.0 μm) was obtained from the z-sliced 3-D scanning images using Imaris Bitplane software. Scale bar=10 μm in upper panels. White squares show the interested areas enlarged below, scale bar=2 μm. (B) The average numbers of STIM1 particles in the whole cell and the perimembranous areas from different groups of cells as indicated are represented as means±SD. n=30-56 cells for each bar. (C) The images show the enhanced STIM1 clustering in CaMKIIδ-overexpressed cells (HA-positive, indicated with arrows) compared with adjacent cells (HA-negative) upon TG (1 μM)+ionomycin (2 μM) stimulation. ** represents P<0.01 vs. control without TG; # and ## stand for P<0.05 and P<0.01 vs. control with TG, respectively, analyzed by one-way ANOVA test.

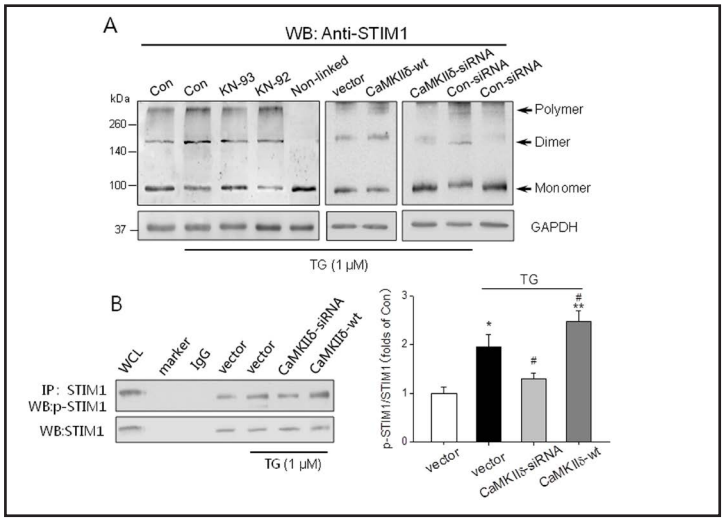

Fig. 7. Effects of CaMKII on STIM1 conformation and serine phosphorylation. (A) Typical blotting bands from 3 independent experiments show the effects of CaMKIIδ gene manipulation on TG-induced STIM1 conformation. HEK293 cells were pretreated with KN-93 (10 μM), KN-92 (10 μM) for 10 min or transfected with CaMKIIδ-wt gene or CaMKIIδ-siRNA for 48 h. Then cells were stimulated with or without 1 μM TG for 5 min in Ca^{2+}-free medium and then cross-linked with 1% formaldehyde for 5 min at room temperature. The cell lysates were separated by 10% SDS-PAGE and subjected to Western blot with anti-STIM1 mouse mAb. (B) Typical blotting bands (left) and statistical data (right) for STIM1 serine-phosphorylation upon TG stimulation. HKE293 cells were transfected with CaMKIIδ-wt or CaMKIIδ-siRNA for 48 h and then stimulated with 1 μM TG in Ca^{2+}-free medium for 5 min. Whole cell lysates were immunoprecipitated with anti-STIM1 mAb and protein-G agarose, and then Western blot was performed with anti-phosphoserine antibody. n=4 independent experiments for each bar. * and ** represents P<0.05 and P<0.01 vs. control without TG; #P<0.05 vs. control with TG, analyzed by one-way ANOVA test.

immunostaining) and confluent (used in the measurement of protein expression by Western blot) HeLa cells were respectively transfected with *CaMKIIδ-wt* at the concentration of 1 μg/ml plasmids, half of the concentration used in other determinations in this study, for 48 h, and then were stimulated with TG+ionomycin. As indicated with arrows in Fig. 6C, HA-positive cells, an indication of CaMKIIδ-wt overexpressed cells, displayed enhanced STIM1 clustering compared with the adjacent HA-negative cells.

Furthermore, STIM1 aggregation was assessed by cross-linking approach with 1% formaldehyde to detect monomers, dimers and polymers. TG caused a reduction in monomers accompanied by an increase in dimmer/polymer forms as already known [5-8]. Unlike cell treated with KN-92, cells treated with KN-93 or CaMKIIδ-siRNA displayed decreased STIM1 aggregation, while cells with CaMKIIδ overexpression showed an increase in dimers/polymers with a decrease in monomers compared with counterpart controls (Fig. 7A).

Finally, the total STIM1 phosphorylation at serine sites was detected to assess if STIM1 phosphorylation was accordingly changed in TG-stimulated cells with different CaMKIIδ manipulation. Here, a pull-down experiment was performed by STIM1 antibody, and a specific anti-phosphoserine antibody was used to detect STIM1 phosphorylation. An increase in Ser-phosphorylation was found in HEK293 cells after TG stimulation, which was down-regulated in CaMKIIδ-knockdown cells, but up-regulated in CaMKIIδ-overexpressed cells (Fig. 7B).

Discussion

CaMKII is an important Ca^{2+} regulatory protein for intracellular Ca^{2+} homeostasis [17-20]. Many studies have shown that CaMKII inhibition causes suppression of SOCE in various types of cells [4, 22, 23, 31, 32]. However, some studies also demonstrate a potentiated effect of CaM and CaMKII inhibition on SOCE [16, 33, 34]. In the present study, we found that pharmacological and siRNA interventions of CaMKII inhibit SOCE, while overexpression of CaMKIIδ up-regulates SOCE in HEK293 and HeLa cells (Figs. 1-3). In addition, STIM1 punctuation and co-localization/interaction with Orai1 were affected by CaMKII inhibition

and CaMKIIδ overexpression (Figs. 4 and 5). Furthermore, STIM1 serine phosphorylation and oligomerization/redistribution onto plasma membrane, and interaction with Orai1 were also altered in accordance to the CaMKII changes [Figs. 6 and 7]. Therefore, these data suggest that CaMKII up-regulates SOCE, at least partly, through targeting STIM1 conformation and interaction with Orai1. Previous reports have mechanically described that CaMKII activation potentiates SOCE by altering SOC channel gating in Xenopus oocytes [31] or enhancing SOC current in multiple types of cells [22, 35]. In accordance with the assessment in SOC channel, we also observed corresponding Ca^{2+} influx change, the final outcome like SOC current in SOCE activation, upon store depletion in different CaMKII manipulated cells. Importantly, we further demonstrated an up-regulation of STIM1 clustering and translocation to plasmalemma by CaMKII, thus activating SOCE.

Physiologically, a small increase in cytosolic Ca^{2+} is sufficient to active CaM and CaMKII, which then provides feedback regulation on Ca^{2+} signal. For instance, activation of CaM upon Ca^{2+} rise acts in concert with STIM1 and the N terminus of Orai1 to evoke rapid SOCE inactivation in many types of cells [16, 34, 36], playing as a down-regulator of SOCE. In contrast, CaMKII activation usually enhances Ca^{2+} signaling; such as promoting ryanodine receptor and L-type Ca^{2+} channel activation in cardiomyocytes [19-21], as well as enhancing SOCE in non-excitable cells [4, 31, 35]. Moreover, CaMKII can be auto-activated in pathological situation [17, 37]. Therefore, the key players, CaM and CaMKII, in Ca^{2+}/CaM/CaMKII pathway can regulate Ca^{2+} signaling independently through CaMKII auto-activation or cooperatively through internal Ca^{2+} increase and act on different target proteins and pathways [17, 34-37], rendering much complicated and fine-tuned Ca^{2+} activities to fit various biological needs in cellular function.

Studies under pathological settings further support up-regulated SOCE by CaMKII. Numerous studies have characterized that Ca^{2+}-handling abnormalities including spontaneous ventricular tachycardia [19, 21], myocardial hypertrophy [22, 38], heart failure [39], neointima formation [23], tumor cell migration/metastasis [4] and cell death [40] are resulted from an increase in CaMKII activity. Similarly, dysfunction of SOCE has been found in diabetic platelets [41, 42], tumor metastasis [43], chondrocyte autophagy [44], and cardiac hypertrophy and arrhythmias [23, 45]. Importantly, some studies have implicated that enhanced CaMKII and SOCE activities are associated with pathological changes [4, 22, 23]. This study provides a direct physiological link between CaMKII and SOCE, and a potential insight into the disturbed Ca^{2+} signaling in pathological condition through their crosstalk.

STIM1 oligomerization triggered by ER Ca^{2+} store depletion is an initial step for SOCE activation. The molecular motif that controls the primary trigger for oligomerization appears to reside in the luminal EF-SAM domains [46]. Once STIM1 oligomerizes, the clustered STIM1 translocates towards the ER-PM junctions and aggregates into puncta. Several phosphorylated residues in STIM1 were found in response to epidermal growth factor stimulation in HeLa cells, but the more detailed physiological connection of these phosphorylations with STIM1 function in SOCE activation remains impalpable [14, 15]. Recent studies have revealed that SOCE is inhibited by phosphorylation of STIM1 in non-excitable cells [15, 47]. Some studies have demonstrated that the phosphorylation of STIM1 in ERK1/2 target serine residues is essential to fully trigger SOCE [14]. Therefore, the exact role of different phosphorylation sites is complicated. In this study, TG treatment increased Ser-phophorylation of STIM1, which was blunted in CaMKII-knockdown cells but enhanced in CaMKII-overexpressed cells, suggesting that CaMKII regulates STIM1 Ser-phosphorylation upon TG stimulation. Therefore, STIM1 phosphorylation at serine sites by CaMKII should be an intermediate process involved in its regulation of SOCE.

Conclusion

This study demonstrates a novel mechanism for CaMKII regulating Ca^{2+} influx through SOC channel. Upon Ca^{2+} store depletion, CaMKII is activated and up-regulates SOCE via

enhancing STIM1 aggregation to the ER-PM contact regions and interaction with Orai1, enabling more Ca^{2+} enter into cytosolic space. As enhanced CaMKII expression and disordered Ca^{2+} signaling are found in many pathologies, such as cardiac hypertrophy and neointima formation, CaMKII upregulation of SOCE through this crosstalk may be one of the mechanisms for its contribution in these pathological processes.

Acknowledgements

This work was supported by grants from the National Natural Science Foundation (81370339, 81570206), Beijing Innovation Promoting Project (TJSHG201510025005), and Beijing Key Laboratory of Metabolic Disorder Related Cardiovascular Disease, Beijing, P.R. China.

Disclosure Statement

No conflict of interests exists.

References

1 Prakriya M, Lewis RS: Store-operated calcium channels. Physiol Rev 2015;95:1383-1436.
2 Putney JWJr, Steinckwich-Besançon N, Numaga-Tomita T, Davis FM, Desai PN, D'Agostin DM, Wu S, Bird G-S: The functions of store-operated calcium channels. Biochimica et Biophysica Acta 2017;1864:900-906.
3 Hulot J-S: A critical role for STIM1 in cardiac hypertrophy. Circ 2011;124:796-805.
4 Umemura M, Baljinnyam E, Feske E-S, De Lorenzo M-S, Xie L-H, Feng X, Oda K, Makino A, Fujita T, Yokoyama U, Iwatsubo M, Chen S, Goydos J-S, Ishikawa Y, Iwatsubo K: Store-operated Ca^{2+} entry regulates melanoma proliferation and cell migration. PLoS One 2014;9:e89292.
5 Lewis R-S: The molecular choreography of a store-operated calcium channel, Nature 2007;446:284-287.
6 Wang Y , Deng X, Zhou Y, Hendron E, Mancarella S, Ritchie M-F, Tang X-D, Baba Y, Kurosaki T, Mori Y, Soboloff J, Gill DL: STIM protein coupling in the activation of Orai channels. Proc Natl Acad Sci USA 2009;106:7391-7396.
7 Shim A-H-R, Tirado-Lee L, Prakriya M: Structural and functional mechanisms of CRAC channel regulation. J Mol Biol 2015;427:77-93.
8 Sharma S, Quintana A, Findlay G-M, Mettlen M, Baust B, Jain M, Nilsson R, Rao A, Hogan P-G: An siRNA screen for NFAT activation identifies septins as coordinators of store-operated Ca^{2+} entry. Nature 2013;499:238-242.
9 Fujii Y, Shiota M, Ohkawa Y, Baba A, Wanibuchi H, Kinashi T, Kurosaki T: Surf4 modulates STIM1-dependent calcium entry. Biochem Biophys Res Commun 2012;422:615-620.
10 Srikanth S, Jung HJ, Kim K-D, Souda P, Whitelegge J, Gwack Y: A novel EF-hand protein, CRACR2A, is a cytosolic Ca^{2+} sensor that stabilizes CRAC channels in T cells. Nat Cell Biol 2010;12:436-446.
11 Palty R, Raveh A, Kaminsky I, Meller R, Reuveny E: SARAF inactivates the store operated calcium entry machinery to prevent excess calcium refilling. Cell 2012;149:425-438.
12 Wang L, Zhang L, Li S, Zheng Y, Yan X, Chen M, Wang H, Putney J-W-Jr, Luo D: Retrograde regulation of STIM1-Orai1 interaction and store-operated Ca^{2+} entry by calsequestrin. Sci Rep 2015;5:113149.
13 Zhang L, Wang L, Li S, Xue J, Luo D: Calsequestrin-1 regulates store-operated Ca^{2+} entry by inhibiting STIM1 aggregation. Cell Physiol Biochem 2016;38:2183-2193.
14 Pozo-Guisado E, Campbell D-G, Deak M, Alvarez-Barrientos A, Morrice N-A, Alvarez IS, Alessi D-, Martín-Romero F-J: Phosphorylation of STIM1 at ERK1/2 target sites modulates store-operated calcium entry. J Cell Sci 2010;123:3084-3093.

15 Sundivakkam P-C, Natarajan V, Malik A-B, Tiruppathi C: Store-operated Ca^{2+} entry (SOCE) induced by protease-activated receptor-1 mediates STIM1 protein phosphorylation to inhibit SOCE in endothelial cells through AMP-activated protein kinase and p38β mitogen-activated protein kinase. J Biol Chem 2013;288:17030-17041.
16 Mullins F-M, Park C-Y, Dolmetsch R-E, Lewis R-S: STIM1 and calmodulin interact with Orai1 to induce Ca^{2+}-dependent inactivation of CRAC channels. Proc Natl Acad Sci USA 2009;106:15495-15500.
17 Bossuyt J, Bers D-M: Visualizing CaMKII and CaM activity: a paradigm of compartmentalized signaling. J Mol Med (Berl) 2013;91:907-916.
18 Wayman G-A, Tokumitsu H, Davare M-A, Soderling T-R: Analysis of CaM-kinase signaling in cells. Cell Calcium 2011;50:1-8.
19 Guo T, Zhang T, Mestril R, Bers D-M: Ca^{2+}/calmodulin-dependent protein kinase II phosphorylation of ryanodine receptor does affect calcium sparks in mouse ventricular myocytes. Circ Res 2006;99:398-406.
20 Grueter C-E, Abiria S-A, DzhuraI I, Wu Y, Ham A-J L, P. Mohler J, Anderson M-E, Colbran R-J: L-type Ca^{2+} channel facilitation mediated by phosphorylation of the beta subunit by CaMKII. Mol Cell 2006;23:641-650.
21 Maier L-S, Bers D-M: Role of Ca^{2+}/calmodulin-dependent protein kinase in excitation-contraction coupling in the heart. Cardiovasc Res 2007;73:631-640.
22 Ji Y, Guo X, Zhang Z, Huang Z, Zhu J, Q. Chen H, Gui L: CaMKIIδ meditates phenylephrine induced cardiomyocyte hypertrophy through store-operated Ca^{2+} entry. Cardiovasc Pathol 2017;27:9-17.
23 Zhang W, Halligan K-E, Zhang X, Bisaillon J-M, Gonzalez-Cobos J-C, Motiani R-K, Hu G, Vincent P-A, Zhou J, Barroso M, Singer H-A, Matrougui K, Trebak M: Orai1-mediated I(CRAC) is essential for neointima formation after vascular injury. Circ Res 2011;109:534-542.
24 Zinchuk V, Wu Y, Grossenbacher-Zinchuk O: Bridging the gap between qualitative and quantitative colocalization results in fluorescence microscopy studies. Sci Rep 2013;3:1365.
25 Costes S-V, Daelemans D, Cho E-H, Dobbin Z, Pavlakis G, Lockett S: Automatic and quantitative measurement of protein-protein colocalization in live cells. Biophys J 2004;86:3993-4003.
26 Grynkiewicz G, Poenie M, Tsien R-Y: A new generation of Ca^{2+} indicators with greatly improved fluorescence properties. J Biol Chem 1985;260:3440-3450.
27 Weerasekera R, She Y-M, Markham K-A, Bai Y, Opalka N, Orlicky S, Sicheri F, Kislinger T, Schmitt-Ulms G: Interactome and interface protocol (2IP): a novel strategy for high sensitivity topology mapping of protein complexes. Proteomics 2007;7:3835-3852.
28 Jardin I, Gómez L-J, Salido G-M, Rosado J-A: Dynamic interaction of hTRPC6 with the Orai1-STIM1 complex or hTRPC3 mediates its role in capacitative or non-capacitative Ca^{2+} entry pathways. Biochem J 2009, 420:267-276.
29 Liu G, Liu G, Chen H, Alzoubi K, Umbach A-T, Gawaz M, Stournaras C, Lang F: Rapid upregulation of Orai1 abundance in the plasma membrane of platelets following activation with thrombin and collagen related peptide. Cell Physiol Biochem 2015;37:1759-1766.
30 Perni S, Dynes J-L, Yeromin A-V, Cahalan M-D, Franzini-Armstrong C: Nanoscale patterning of STIM1 and Orai1 during store-operated Ca^{2+} entry, Proc Natl Acad Sci USA 2015;112:E5533-5542.
31 Machaca K: Ca^{2+}-calmodulin-dependent protein kinase II potentiates store-operated Ca^{2+} current. J Biol Chem 2003;278:33730-33737.
32 McElroy S-P, Drummond R-M, Gurney A-M: Regulation of store-operated Ca^{2+} entry in pulmonary artery smooth muscle cells. Cell Calcium 2009;46:99-106.
33 Matifat F, Fournier F, Lorca T, Capony J-P, Brûlé G, Collin T-T: Involvement of the Ca^{2+}/calmodulin-dependent protein kinase II pathway in the Ca^{2+}-mediated regulation of the capacitative Ca^{2+} entry in Xenopus oocytes. Biochem J 1997;322:267-272.
34 Li X, Wu G, Yang Y, Fu S, Liu X, Kang H, Yang X, Su X-C, Shen Y: Calmodulin dissociates the STIM1-Orai1 complex and STIM1 oligomers. Nat Commun 2017;8:1042.
35 Shi J, Mori E, Mori Y, Mori M, Li J, Ito Y, Inoue R: Multiple regulation by calcium of murine homologues of transient receptor potential proteins TRPC6 and TRPC7 expressed in HEK293 cells. J Physiol 2004;561(Pt 2):415-432.
36 Bauer M-C, O'Connell D, Cahill D-J, Linse S: Calmodulin binding to the polybasic C-termini of STIM proteins involved in store-operated calcium entry. Biochem 2008;47:6089-6091.
37 Feng N, Anderson M-E: CaMKII is a nodal signal for multiple programmed cell death pathways in heart. J Mol Cell Cardiol 2017;103:102-109.

38 Subedi K-P, Son M-J, Chidipi B, Kim S-W, Wang J, Kim K-H, Woo S-H, Kim J-C. Signaling pathway for endothelin-1- and phenylephrine-induced cAMP response element binding protein activation in rat ventricular myocytes: role of inositol 1, 4,5-trisphosphate receptors and CaMKII. Cell Physiol Biochem 2017;41:399-412.

39 Sossalla S, Fluschnik N, Schotola H, Ort K-R, Neef S, Schulte T, Wittköpper K, Renner A, Schmitto J-D, Gummert J, El-Armouche A, Hasenfuss G, Maier L-S: Inhibition of elevated Ca^{2+}/calmodulin-dependent protein kinase II improves contractility in human failing myocardium. Circ Res 2010;107:1150-1161.

40 Wang Q, Huang L, Yue J: Oxidative stress activates the TRPM2-Ca^{2+}-CaMKII-ROS signaling loop to induce cell death in cancer cells. Biochimica et Biophysica Acta 2017;1864:957-967.

41 Zhu Z, Zhou H, Yu X, Chen L, Zhang H, Ren S, Wu Y, Luo D: Potential regulatory role of calsequestrin in platelet Ca^{2+} homeostasis and its association with platelet hyperactivity in diabetes mellitus. J Thromb Haemost 2012;10:116-124.

42 Xia W, Li Y, Wang B, Chen J, Wang X, Sun Q, Sun F, Li Z, Zhao Z: Enhanced store-operated calcium entry in platelets is associated with peripheral artery disease in type 2 diabetes. Cell Physiol Biochem 2015;37:1945-1955.

43 Xie J, Pan H, Yao J, Zhou Y, Han W: SOCE and cancer: Recent progress and new perspectives. Int J Cancer 2016;138:2067-2077.

44 Wei Y, Wang Y, Wang Y, Bai L: Transient receptor potential vanilloid 5 mediates Ca^{2+} influx and inhibits chondrocyte autophagy in a rat osteoarthritis model. Cell Physiol Biochem 2017;42:319-332.

45 Collins H-E, Zhu-Mauldin X, Marchase R-B, Chatham J-C: STIM1/Orai1-mediated SOCE: current perspectives and potential roles in cardiac function and pathology. Am J Physiol Heart Circ Physiol 2013;305:H446-458.

46 Stathopulos P-B, Zheng L, Li G-Y, Plevin M-J, Ikura M: Structural and mechanistic insights into STIM1-mediated initiation of store-operated calcium entry. Cell 2008;135:110-122.

47 Smyth J-T, Petranka J-G, Boyles R-R, DeHaven W-I, Fukushima M, Johnson K-L, Williams J-G, Putney J-W-Jr: Phosphorylation of STIM1 underlies suppression of store-operated calcium entry during mitosis. Nat Cell Biol 2009;11:1465-1472.